Precursor diamagnetism in layered and isotropic superconductors*†

Rolf R. Gerhardts‡
Department of Applied Physics, Stanford University, Stanford, California 94305
(Received 30 July 1973)

The theory of diamagnetic fluctuations in a system of Josephson-coupled superconducting layers is studied using the approach of Kurkijärvi, Ambegaokar, and Eilenberger, but with a modified treatment of finite frequency fluctuations proposed by Maki and Takayama. Both temperature and field dependence of the fluctuation-induced magnetization above T_c are discussed. The results are extended to the limit of isotropic superconductors, where they are generally in good agreement with the experimental results of Gollub, Beasley, and Tinkham, for both clean and dirty superconductors. For weakly coupled layers, the temperature dependence of the magnetization for fixed field changes from a $[T-T_c(B)]^{-1/2}$ behavior near the phase transition, typical of three-dimensional superconductors, to a $[T-T_c(B)]^{-1}$ behavior of two-dimensional character at higher temperatures, as predicted by Lawrence and Doniach, Similarly, the field dependence at T_c changes from a $\sqrt{B}$ dependence to a relatively field-independent behavior at higher fields. With increasing layer coupling, these changes take place at higher temperatures and fields, respectively, but they are masked by effects which suppress fluctuations at high fields and temperatures. The numerical results are consistent with the layer-compound data of Prober, Beasley, and Schwall, but they show that these compounds behave much more like three-dimensional than like two-dimensional systems, in spite of the apparent Curie-Weiss–like temperature dependence of the susceptibility.

I. INTRODUCTION

Recently, the precursor diamagnetism of superconducting layer compounds, transition-metal dichalcogenides intercalated with organic molecules, has been investigated experimentally by Geballe *et al.*,[1] and by Prober, Beasley, and Schwall (PBS).[2] In a magnetic field perpendicular to the layer planes, the enhanced susceptibility, caused by superconducting fluctuations in the normal state, showed a Curie-Weiss–type behavior, $\Delta\chi \sim (T-T_c)^{-1}$ within a certain material-dependent temperature region, which was interpreted as indication of a two-dimensional nature of the fluctuations.

A susceptibility formula derived by Lawrence and Doniach[3] for layer-compound superconductors indeed predicts a Curie-Weiss–type behavior well above T_c, and a three-dimensional behavior $\Delta\chi \sim (T-T_c)^{-1/2}$ near T_c, where the Ginzburg-Landau coherence length exceeds the spacing of the metallic layers. The Lawrence-Doniach formula was based on the theory of static fluctuations of the Ginzburg-Landau order parameter worked out by Schmid[4] and by Schmidt,[5] and it interpolates between Schmid's results for three-dimensional and for two-dimensional superconductors.

Extensive experimental work by Gollub, Beasley, and Tinkham (GBT)[6] on several isotropic superconductors has shown, however, that the Schmid theory, which has been worked out explicitly for finite magnetic field by Prange,[7] is not sufficient to describe the experimental results adequately. With increasing temperature and magnetic field the measured susceptibility is progressively depressed below the Schmid-Prange result. This had been predicted by Patton, Ambegaokar, and Wilkins (PAW),[8] who invented a phenomenological cutoff to suppress high-energy fluctuations which are overestimated by the simple Schmid theory. Subsequent theoretical work by Lee and Payne (LP),[9] by Kurkijärvi, Ambegaokar, and Eilenberger (KAE),[10] and by Maki and Takayama (MT)[11] attributed the dominant cut-off mechanism to nonlocal electrodynamics for clean superconductors and to finite frequency fluctuations for dirty superconductors.

Of course, these nonlocal and dynamic effects must be expected to be important for layer compounds, too. It is the purpose of the present paper to calculate the fluctuation susceptibility for layer-compound superconductors with arbitrary concentration of impurities, starting from a microscopic model and including both types of cut-off effects. The result should provide a reliable basis for the interpretation of experiments.

In many respects, the present approximate evaluation of the magnetization closely follows the treatment of impure superconductors given by KAE. But there are two important differences. First, in the basic Gorkov Hamiltonian the single-particle energy for the motion perpendicular to the layer planes is replaced by a Josephson-type interlayer coupling, as was proposed by Lawrence and Doniach.[12] Second, the final sum over the frequencies of the pair fluctuations is evaluated according to the procedure proposed by MT.[11]

The model used is applicable to isotropic three-

dimensional (3D) superconductors as a limiting case. This provides a useful test of the numerical results. The 3D curves for the field dependence of the magnetization at $T = T_c$ scale with great accuracy to a single one, if the field is measured in units of a scaling field B_s. The values of B_s are in reasonable agreement with the experimental values[6] for all impurity concentrations. The experimentally observed universal behavior of the temperature dependence of the magnetization for fixed magnetic field, $B/B_s = \text{const}$, is also reproduced very closely for low fields, $B/B_s \sim 0.3$. For high fields, $B/B_s \sim 5$, only experimental data on clean superconductors are available, and the theoretical result for low impurity concentration is in good agreement with these data. The result for the dirty limit differs noticeably from that for the clean limit, indicating a breakdown of universal behavior at high magnetic field.

Comparison of the corresponding results for layer compounds with experiments was not possible, since no data on the field dependence exist, and, therefore B_s is not known experimentally. In general, the theoretical results look very similar to those of the 3D limit, except for extremely small interlayer coupling.

The dirty limit results of the present theory are in close agreement with results obtained very recently by Klemm *et al.*,[13] who applied a slightly improved version of the MT dirty-limit calculations to the case of layer compounds, replacing the pair energy by the tight-binding form proposed by Lawrence and Doniach.

To make a comparison with the experiments of PBS possible, the temperature dependence of the zero-field susceptibility is also investigated in this paper. For this case, Klemm presents theoretical results for the 3D limit only, and he reports results of an extrapolation to zero field of data on an isotropic Pb-Tl alloy to zero temperatures. He reports that these can be represented by the same curve as the data of PBS. In the 3D limit, the numerical results of the present theory for low impurity concentration are in good agreement with the experimental data, whereas the dirty-limit results differ noticeably from these, and agree well with Klemm's calculation. The layer-compound results show that, for the values of the material parameters referring to the PBS samples, the theoretical susceptibility differs only very slightly from the 3D limit. This is in agreement with the experimental data reported by Klemm and shows that the Curie-Weiss–type behavior of the susceptibility is not a conclusive indication of 2D fluctuations. However, we will show below that the magnitude of the scaling field B_s does provide a very direct indication of the transition towards quasi-2D behavior as the interlayer coupling is reduced by intercalation.

The theory also indicates that a layer-compound superconductor with an interlayer coupling, which is only one order of magnitude smaller than that of the TaS_2 (pyridine)$_{1/2}$ investigated by PBS, should show a noticeable deviation from 3D behavior for temperatures in the regime $T_c < T \lesssim 1.2T_c$. Thus, experiments with compounds of larger layer spacing are very promising in this respect.

Another question, which requires further clarification, both experimentally and theoretically, is the mentioned breakdown of universal behavior. If further experiments should prove universality, the adequacy of calculations based on the MT summation procedure has to be questioned.

The analysis leading to the generalized Ginzburg-Landau theory of the normal state and an expression for the fluctuation-enhanced magnetization is the subject of Sec. II. In Sec. III the results of the numerical calculations are discussed and compared with experiments and other theories. Finally, Appendix A contains some mathematical details concerning the symmetry properties of the pair propagator, and in Appendix B the validity of the MT summation procedure for superconductors with arbitrary concentration of impurities is discussed.

II. ANALYSIS

A. Model Hamiltonian and free energy

Following Lawrence and Doniach,[3,12] we describe the conduction electrons of a layer-compound superconductor by a Hamiltonian which treats the electrons within a metallic layer in the effective-mass approximation and couples neighboring layers by a Josephson-type term.

In the presence of a homogenous magnetic field $\vec{B} = \vec{\nabla} \times \vec{A}$ perpendicular to the layer planes, this Hamiltonian can be written

$$H_0 = \sum_{j,\sigma} \int d^2x \left[\frac{1}{2m} \psi^{\dagger}_{j,\sigma}(\vec{x}) \left(\frac{\hbar}{i} \partial_{\vec{x}} + \frac{|e|}{c} \vec{A}(\vec{x}) \right)^2 \times \psi_{j\sigma}(\vec{x}) - \tfrac{1}{2}\eta \psi^{\dagger}_{j,\sigma}(\vec{x}) (\psi_{j+1,\sigma}(\vec{x}) - 2\psi_{j,\sigma}(\vec{x}) + \psi_{j-1,\sigma}(\vec{x})) \right] , \quad (2.1)$$

where the vectors $\vec{x}$, $\partial_{\vec{x}}$, $\vec{A}$ act in the x-y plane and the index j, labeling the layers, substitutes for the z variable $z = sj$, with s, the layer spacing. In this model, the z dependence of the single-particle states has a tight-binding form, and for vanishing magnetic field the single-particle energy is

$$\epsilon(\vec{k}) = (\hbar^2/2m)(k_x^2 + k_y^2) + \eta(1 - \cos s k_z) , \quad (2.2)$$

where $|k_z| \leq \pi/s$. Expanding for small k_z, we can express $\eta = \hbar^2/M_{\perp} s^2$ in terms of the effective mass $M_{\perp}$ in the z direction.

To describe the effective electron-electron interaction, we write

$$H_1 = -\lambda \sum_j \int d^2x\, \psi^\dagger_{j,\uparrow}(\vec{x})\psi^\dagger_{j,\downarrow}(\vec{x})\psi_{j,\downarrow}(\vec{x})\psi_{j,\uparrow}(\vec{x}) \,. \quad (2.3)$$

As usual, this attractive interaction will be allowed to act only on particles within a shell of width $\hbar\omega_D$ about the Fermi surface.

It is only through the parameters η and λ that the model Hamiltonian $H = H_0 + H_1$ contains information about the nonmetallic constituents of the layer compound, such as intercalating organics.

For mathematical convenience we introduce the notation

$$\psi_{js\sigma}(\vec{x})/\sqrt{s} = \psi_\sigma(\vec{r}) \,, \quad \vec{r} = (x, y, z = sj) \,, \quad \lambda s = \bar{\lambda} \,,$$

and

$$\int_r = \int dx \int dy\, s \sum_j \,,$$

and rewrite the Hamiltonian in the compact form

$$H = \sum_\sigma \int_r \psi^\dagger_\sigma(\vec{r}) \epsilon\left(\frac{\hbar}{i}\vec{\nabla} + \frac{|e|}{c}\vec{A}(\vec{r})\right)\psi_\sigma(\vec{r}) - \bar{\lambda}\int_r \psi^\dagger_\uparrow(\vec{r})\psi^\dagger_\downarrow(\vec{r})\psi_\downarrow(\vec{r})\psi_\uparrow(\vec{r}) \,. \quad (2.4)$$

For fixed $M_\perp$ and vanishing layer spacing s, this reduces to the usual three-dimensional form of the Gorkov Hamiltonian.[9,10]

For $\eta = 0$, it describes the 2D limit of decoupled layers, and may also be reinterpreted as a model for a thin film of thickness s.[13]

To calculate the enhanced diamagnetism due to the effective electron-electron interaction (2.3), i.e., due to fluctuations of the order parameter, we follow the approach of Lee and Payne[9] and write the grand canonical free energy

$$\Omega(\lambda) = -(1/\beta)\ln \mathrm{Tr}\, e^{-\beta(H-\mu N)} \quad (2.5)$$

in terms of the pair propagator

$$L(\vec{r}, t; \vec{r}', t') = -T\langle \psi_\uparrow(\vec{r}, t)\psi_\downarrow(\vec{r}, t) \times \psi^\dagger_\downarrow(\vec{r}', t')\psi^\dagger_\uparrow(\vec{r}', t')\rangle \,, \quad (2.6)$$

which is evaluated in the ladder approximation.[14] But we want to point out that the analysis can be greatly simplified by taking advantage of the cylindrical symmetry of the model. Because of this symmetry, the single-particle Green's function is diagonal in the Landau representation, as is well known,[15] and, furthermore, the exact pair propagator (2.6) is diagonal in the Landau representation for a particle of charge $2e$.

These consequences of the symmetry properties and the resulting simplified analysis are discussed in more detail in Appendix A.

In the ladder approximation we obtain, for the contribution of fluctuations to the free energy,

$$\delta\Omega = \Omega(\lambda) - \Omega(0) = \frac{V}{2\pi^2 R^2 \beta}\sum_{\nu=-\infty}^{\infty}\sum_{n=0}^{\infty}\int dk_z \ln[1 - \bar{\lambda}\Pi_{nk_z}(\nu)] \quad (2.7)$$

with $R = (|e|B/\hbar c)^{-1/2}$ the magnetic length, V is the volume, and

$$\Pi_{nk_z}(\nu) = \frac{1}{\beta}\sum_l \{Q_{nk_z}(\nu, l)^{-1} - \hbar/[2\pi\tau N(\mu)]\}^{-1} \,. \quad (2.8)$$

Here the effect of impurities is described in terms of the scattering lifetime τ. $N(\mu)$ is the density of states at the Fermi surface, and Q is the product of impurity averaged single-particle Green's functions in the representation Ψ_α, which diagonalizes the pair propagator:

$$Q_{nk_z}(\nu, l) = \int_{\vec{r}}\int_{\vec{r}'} \Psi^*_\alpha(\vec{r})G^0_\uparrow(\vec{r}, \vec{r}'; \zeta_l) \times G^0_\downarrow(\vec{r}, \vec{r}'; \zeta_{\nu-l-1})\Psi_\alpha(\vec{r}') \,, \quad (2.9)$$

with (cf. Appendix)

$$\zeta_l = \mu + i\,\mathrm{sgn}(2l+1)(|2l+1|\pi/\beta + \hbar/2\tau).$$

This formula still contains the full magnetic field dependence. But for magnetic field values of practical interest, the cyclotron energy is much smaller than $2\pi kT + \hbar/\tau$—even for clean superconductors at the transition temperature—and, therefore, we use the semiclassical approximation

$$G^0(\vec{r}, \vec{r}'; \zeta_l) = \exp\left(-i\frac{|e|}{2c\hbar}(\vec{r} - \vec{r}')\cdot\vec{A}(\vec{r} + \vec{r}')\right) \times G^0(\vec{r} - \vec{r}'; \zeta_l; B = 0) \,, \quad (2.10)$$

neglecting the field dependence, which could lead to oscillatory effects of the de Haas–van Alphen type. We then obtain

$$Q_{nk_z}(\nu, l) = (-1)^n \int_0^\infty dx\, e^{-x} L_n(2x) \times Q(2x/R^2, k_z; \nu, l) \,, \quad (2.11)$$

where L_n is a Laguerre polynominal and

$$Q(q_x^2 + q_y^2, q_z; \nu, l) = \int \frac{d^3k}{(2\pi)^3}\frac{1}{\zeta_l - \epsilon(\vec{k})}\frac{1}{\zeta_{\nu-l-1} - \epsilon(\vec{q} - \vec{k})} \,. \quad (2.12)$$

This differs from the corresponding formulas given by LP and by KAE only through the different single-particle energy $\epsilon(\vec{k})$.

B. Evaluation of the pair propagator

In the calculation of the magnetization from the free energy, we will not attempt to use the full result for the eigenvalues Π_α, given by Eqs. (2.8), (2.11), and (2.12), since this would require a very complex numerical work. Instead of this, we make two kinds of approximations, both in the spirit of the work of KAE.

KAE have investigated the role of the "nonlocal"

effects which cause the difference between Eq. (2.11) and its local approximation

$$Q^{\rm loc}_{nk_z}(\nu, l) = Q[(4n+2)/R^2, k_z; \nu, l] \ . \qquad (2.13)$$

They found that the full nonlocal result for the magnetization is very closely reproduced, if one evaluates the derivative with respect to the magnetic field B using the difference formula

$$2B\frac{\partial}{\partial B} Q_{nk_z} = (n+1)Q_{n+1\,k_z} - Q_{nk_z} - nQ_{n-1\,k_z} \ , \qquad (2.14)$$

and then replaces the nonlocal Q_{nk_z} by its local approximation $Q^{\rm loc}_{nk_z}$. We will adopt this approximation in the following. As a second type of approximation, we will replace the results of Eqs. (2.12) and (2.8) by simpler expressions which behave correctly in the limit of long-wavelength–low-frequency fluctuations, but allow the k_z integral in Eq. (2.7) to be evaluated analytically. As a result of this only the final frequency summation and the sum over the Landau quantum numbers n in Eq. (2.7) need to be carried out numerically. Lee and Payne discussed in some detail how Eq. (2.12) can be evaluated approximately in the isotropic three-dimensional case, and under which condition this approximation is meaningful ($\omega_D \tau \gg 1$). Applying the same kind of approximation we obtain

$$Q(q_x^2+q_y^2, q_z; \nu, l) = \int \frac{d^2k_\parallel}{(2\pi)^2} \int_{-\pi/s}^{\pi/s} \frac{dk_z}{2\pi} \frac{2\pi i \,\mathrm{sgn}(2l+1)\Theta(-(2l+1)(2\nu-2l-1))}{\zeta_l - \zeta_{\nu-l-1} - [\epsilon(\vec{k}+\frac{1}{2}\vec{q}) - \epsilon(\vec{k}-\frac{1}{2}\vec{q})]} \delta(\mu - \epsilon(\vec{k})) \ , \qquad (2.15)$$

with $\epsilon(\vec{k})$ given by Eq. (2.2) and $\Theta(x)$ the step function. This can be simplified to

$$Q(q_\parallel^2, q_z; \nu, l) = \frac{m}{s} \frac{\Theta(-(2l+1)(2\nu-2l-1))}{|\zeta_l - \zeta_{\nu-l-1}|} \times \int_{-\pi}^{\pi} \frac{dz}{2\pi} \left\{ \Theta(\mu - \eta(1-\cos z)) \Big/ \left[\left(1 - \frac{2\eta \sin z \sin(\frac{1}{2}sq_z)}{\zeta_l - \zeta_{\nu-l-1}} \right)^2 + \frac{2}{m}\hbar^2 q_\parallel^2 \frac{\mu - \eta(1-\cos z)}{|\zeta_l - \zeta_{\nu-l-1}|^2} \right]^{1/2} \right. \ , \qquad (2.16)$$

which integrates exactly in the 3D limit ($s^2\eta = \hbar^2/M_\perp$ fixed, $s \to 0$), in the 2D limit ($\eta = 0$), and in the special cases $q_\parallel = 0$ or $q_z = 0$, but not in the general case. Therefore, we evaluated Eq. (2.16) for small $\epsilon(\vec{q})$ to obtain the approximate result

$$Q(q_\parallel^2, q_z; \nu, l) = 2\pi N(\mu) \frac{\Theta(-(2l+1)(2\nu-2l-1))}{|\zeta_l - \zeta_{\nu-l-1}|} \left(1 + \frac{4}{d} \frac{\mu \tilde{\epsilon}(\vec{q})}{|\zeta_l - \zeta_{\nu-l-1}|^2} \right)^{-1} \ , \qquad (2.17)$$

with

$$\tilde{\epsilon}(\vec{q}) = (\hbar^2/2m)(q_x^2+q_y^2) + \tilde{\eta}(1-\cos q_z s) \ . \qquad (2.18)$$

$\frac{1}{2}\tilde{\epsilon}(\vec{q})$ may be considered as energy of a pair fluctuation with momentum $\hbar\vec{q}$ and effective masses $2m$ and $2\tilde{M}_\perp$.

In terms of the auxiliary functions

$$f_0(x) = \Theta(1-x) + \frac{1}{\pi}\Theta(2x-1)\arctan\frac{(2x-1)^{1/2}}{x-1} \ ,$$

$$f_\perp(x) = f_0(x) + \frac{1}{\pi}\Theta(2x-1)\frac{1-x}{x^2}(2x-1)^{1/2} \ ,$$

$$f_\parallel(x) = (1-x)\Theta(1-2x) + \frac{1}{\pi}\Theta(2x-1) \times \left((2x-1)^{1/2} + 2(1-x)\arctan\frac{1}{(2x-1)^{1/2}} \right) , \qquad (2.19)$$

the density of states at the Fermi surface is given by

$$N(\mu) = (m/2\pi s) f_0(\eta/\mu) \ , \qquad (2.20)$$

the "pair" coupling parameter $\tilde{\eta}$ by

$$\tilde{\eta}/\eta \equiv M_\perp/\tilde{M}_\perp = \frac{1}{2}\frac{\eta}{\mu} f_\perp\left(\frac{\eta}{\mu}\right) \Big/ f_\parallel\left(\frac{\eta}{\mu}\right) \ , \qquad (2.21)$$

and d by

$$d = 2f_0(\eta/\mu)/f_\parallel(\eta/\mu) \ . \qquad (2.22)$$

Figure 1 shows a plot of $N(\mu)$, $\tilde{\eta}/\eta$, and d vs η/μ. In the three-dimensional limit $d = 3$, and Eq. (2.17) is equivalent to the approximation used by KAE [cf. their Eq. (4.6)].

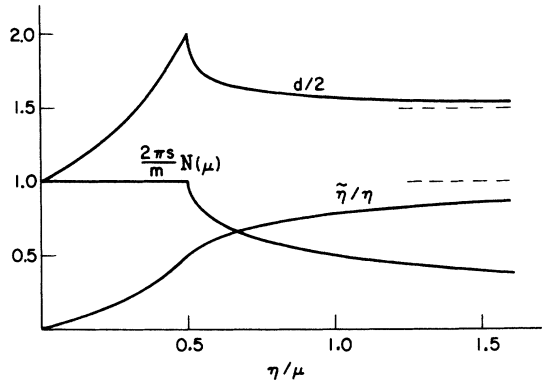

FIG. 1. Density of states at the Fermi level $N(\mu)$, interlayer pair-coupling parameter $\tilde{\eta}$, and the variable d, related to the dimensionality of the system, as functions of interlayer coupling η.

Following the notation of KAE, we define the coherence length $\xi_0 = \hbar v_F \beta/2\pi$, the reduced magnetic field $b = \xi_0^2/R^2 = (|e|B/\hbar c)\xi_0^2$, and $\rho = \xi_0/v_F\tau$ measuring the impurity concentration.

Then, using Eq. (2.17), we can evaluate Eq. (2.8) to yield

$$\Pi_{nk_z}(\nu) = 2N(\mu)\sum_{l=0}^{\Lambda/2}[I_{nk_z}(l,\nu)^{-1} - \rho]^{-1}\,, \tag{2.23}$$

with I given in the local approximation by

$$I^{\rm loc}_{nk_z}(l,\nu)^{-1} = 2l + 1 + |\nu| + \rho + \frac{2}{d}\,\frac{2b(n+\frac{1}{2}) + (m\xi_0^2/\tilde{M}s^2)(1-\cos sk_z)}{2l+1+|\nu|+\rho} \tag{2.24}$$

and with $\Lambda = \hbar\omega_D\beta/\pi$ the cut-off parameter of the BCS theory. Strictly speaking, Eq. (2.23) is applicable only for $|\nu| \ll \frac{1}{2}\Lambda$, but since only small ν will contribute significantly to our final result, we can ignore this restriction.

With the standard BCS relation

$$1 = \bar{\lambda}N(\mu)\left[\psi\left(\frac{\hbar\omega_D}{2\pi kT_c}\right) - \psi(\tfrac{1}{2})\right] \approx \bar{\lambda}N(\mu)\ln\left(\frac{\gamma\hbar\omega_D}{kT_c}\right), \tag{2.25}$$

ψ being the digamma function, the argument of the logarithm in Eq. (2.7) can be written

$$E_{nk_z}(\nu) = 1 - \bar{\lambda}\Pi_{nk_z}(\nu) = \bar{\lambda}N(\mu)\left[\ln\frac{T}{T_c} + 2\sum_{l=0}^{\Lambda/2}\left(\frac{1}{2l+1} - \frac{1}{I^{-1}_{nk_z}(l,\nu)-\rho}\right)\right]. \tag{2.26}$$

In their calculation of the magnetization for finite ρ at $T = T_c$, KAE simply dropped the terms with $l > 0$. Since this leads to a completely unphysical result for $H_{c2}(T)$ at low temperatures, we use a slightly different approximation. Omitting the l dependence of the denominator in Eq. (2.24), we can easily evaluate $E_{nk_z}(\nu)$. To simplify the result further, we follow MT[11] and define $\epsilon(T)$ by the relation

$$\ln\frac{T}{T_c} + \psi\left(\frac{1}{2} - \frac{\epsilon(T)}{4\pi kT}\right) - \psi(\tfrac{1}{2}) + \left[\psi\left(\frac{\Lambda-1}{2}\right) - \psi\left(\frac{\Lambda-1}{2} - \frac{\epsilon(T)}{4\pi kT}\right)\right] = 0\,. \tag{2.27}$$

Here the term within the square brackets is negligibly small, since $\Lambda \gg 1$ for $T = T_c$. Then, using Eqs. (2.25)–(2.27) and an approximation of the type

$$\sum_{l=0}^{\Lambda/2}\frac{1}{l+\frac{1}{2}(z+1)} = \psi\left(\frac{\Lambda-1+z}{2}\right) - \psi\left(\frac{1+z}{2}\right) \approx \frac{\psi(\frac{1}{2}(\Lambda-1-\epsilon)) - \psi(\frac{1}{2}(1-\epsilon))}{1+\frac{1}{2}Q(\epsilon+z)}\,,$$

we finally obtain the interpolation formula

$$E^{\rm loc}_{nk_z}(\nu) = 1 - \left[1 + \frac{Q}{2}\left(\frac{\epsilon(T)}{2\pi kT} + |\nu| + \frac{b(4n+2) + 2(m\xi_0^2/\tilde{M}_\perp s^2)(1-\cos sk_z)}{d(1+|\nu|+\rho)}\right)\right]^{-1} \tag{2.28}$$

with

$$Q(T) = \bar{\lambda}N(\mu)\left[\psi'\left(\frac{1}{2} - \frac{\epsilon(T)}{4\pi kT}\right) - \psi'\left(\frac{\Lambda-1}{2} - \frac{\epsilon(T)}{4\pi kT}\right)\right]. \tag{2.29}$$

If we expand Eq. (2.27) for small Q and keep only the linear term, we obtain essentially the approximation of $E_{nk}(\nu)$, which was used by MT. But in addition, Eq. (2.28) takes into account that Π_{nk_z} has to vanish for large quantum numbers n (or $q_\parallel^2$). For temperatures near T_c, we find from Eqs. (2.25) and (2.29) that for a typical weak-coupling superconductor Q is in the range $1 \lesssim Q(T_c) \lesssim 2$ showing only a very weak dependence on the BCS cutoff Λ.

In fact, for $T = T_c$ and $Q = 2$, Eq. (2.28) is equivalent to the approximation used by KAE in the impure case. Numerical calculations have shown that in the clean limit the results of the present theory (more explicitly, of the nonlocal static approximation defined in Sec. II C) agree best with the results of the more rigorous 3D clean-limit calculations by LP and KAE, if we choose $Q = 2$. Furthermore, since our final results depend only weakly on Q for impurity concentrations with $\rho \gtrsim 3$, we discuss, in the following, only the results for $Q(T_c) = 2$.

C. Magnetization formula

First, we consider the magnetization in the local approximation. If we insert Eq. (2.28) into the free-energy formula, Eq. (2.7), we find that the sum over the Landau quantum numbers n diverges. This kind of divergence was reported and discussed in Refs. 7 and 9–11. It always occurs, if one treats the conduction electrons as free electrons and describes their interaction by a δ function in the position space. To circumvent this difficulty, one can either use a more realistic interaction potential of finite range, or restrict the electrons to a conduction band of finite width. But, as already noticed by Prange,[7] one does not really need such an improved theory to calculate the magnetization, since the divergent contribution to the free energy is independent of the magnetic field in the following sense. In the local approximation we can write

$$\delta\Omega(B)-\delta\Omega(0)=V\frac{|e|BkT}{2\pi^2\hbar c}\sum_{\nu=-\infty}^{\infty}\sum_{n=0}^{\infty}\int dk_z\left(\ln E^{\rm loc}_{nk_z}(\nu)-\int_n^{n+1}dx\ln E^{\rm loc}_{(x-1/2)\,k_z}(\nu)\right), \tag{2.30}$$

where the sum over n simply extends the x integration in the subtracted terms from 0 to ∞. Thus, the substitution $Bx=y$ shows that the subtracted term is independent of the magnetic field and, in fact, is the zero-field contribution to the free energy.

In Eq. (2.30) the n sum is convergent (and also the k_z integral—even in the 3D limit), and we can use this formula to calculate the magnetization. The result is

$$\delta M^{\rm loc}=-V\frac{|e|kT}{2\pi^2\hbar c}\sum_{\nu=-\infty}^{\infty}\sum_{n=0}^{\infty}\int_{-\pi/s}^{\pi/s}dk_z\left\{\ln E_{nk_z}+\frac{B}{E_{nk_z}}\frac{\partial E_{nk_z}}{\partial B}-[(n+1)\ln E_{(n+1/2)\,k_z}-n\ln E_{(n-1/2)\,k_z}]\right\} \tag{2.31}$$

with $E_{nk_z}=E^{\rm loc}_{nk_z}(\nu)$ given by Eq. (2.28). Equation (2.31) can be written precisely in the form in which Prange[7] presented his result. Using Eq. (2.28), we can carry out the k_z integration in Eq. (2.31) exactly.

We obtain

$$-\frac{\delta M^{\rm loc}4\pi}{VkT\sqrt{B}}\left(\frac{\hbar c}{4|e|}\right)^2=\left(\frac{\tilde M_\perp}{m}\right)^{1/2}\sum_{\nu=-\infty}^{\infty}y^{1/2}[F(x_\nu,y)-F(x_\nu+z_\nu,y)], \tag{2.32}$$

with

$$y=(m/\tilde M_\perp)(\xi_0/s)^2/b\,,\quad x_\nu=(|\nu|+\epsilon(T)\beta/2\pi)(1+|\nu|+\rho)d/4b\,,\quad z_\nu=(1+|\nu|+\rho)d/(2Qb)\,,$$

and

$$F(x,y)=\frac{1}{8w_0^+}+\frac{1}{4}\sum_{n=1}^{\infty}\left(\frac{n+\frac12}{w_n^+}+\frac{n-\frac12}{w_n^-}-2n\ln\frac{n+\frac12+x+\frac12y+w_n^+}{n-\frac12+x+\frac12y+w_n^-}\right), \tag{2.33}$$

where

$$w_n^\pm(x)=[n\pm\tfrac12+x+y)(n\pm\tfrac12+x)]^{1/2}\,.$$

From Eq. (2.33) one can show that

$$\lim_{y\to\infty}\sqrt{y}F(x,y)=f_{\rm Prange}(x)\,. \tag{2.34}$$

Thus, the first term in the square brackets of Eq. (2.32) with $\nu=0$ corresponds to the Prange approximation. To obtain an approximation which is essentially that of MT,[11] we have to include the frequency dependence of this term (the main difference being that we include a "frequency-dependent diffusion constant" which makes the frequency sum convergent). The last term in Eq. (2.32) arises from the fact that we have used Eq. (2.28), and not only its linear approximation. This leads to a cutoff similar to the one introduced phenomenologically by PAW.[8] But the numerical calculations show that this cutoff is in no case the most important one.

To include nonlocal effects according to the approximation discussed in Sec. II B we have to replace the second term in the curly brackets of Eq. (2.31) by the one obtained by evaluating the derivative with respect to B according to the difference formula, Eq. (2.14). To this end, we calculate $B(\partial/\partial B)E_{nk_z}$ from Eq. (2.26) and apply Eq. (2.14) to I_{nk_z} given by Eq. (2.24), where the l dependence of the denominator again is omitted. We then evaluate the l sums, using the approximation

$$\sum_{l=0}^{\Lambda/2}\left(l+\frac{1+z}{2}\right)^{-2}=-2\frac{d}{dz}\sum_{l=0}^{\Lambda/2}\left(l+\frac{1+z}{2}\right)^{-1}\approx\left[\psi\left(\frac{\Lambda-1-\epsilon}{2}\right)-\psi\left(\frac{1-\epsilon}{2}\right)\right]\frac{Q}{[1+\frac12Q(\epsilon+z)]^2}$$

and obtain an interpolation formula for the nonlocal correction, which is consistent with Eq. (2.28), and which allows the k_z integration to be carried out analytically. The final result can be written in the form

$$-\frac{\delta M^{\rm nl}4\pi}{VkT\sqrt{B}}\left(\frac{\hbar c}{4|e|}\right)^{3/2}=\left(\frac{\tilde M_\perp}{m}\right)^{1/2}\sum_{\nu=-\infty}^{\infty}\sqrt{y}[C(x_\nu,x_\nu+z_\nu+r_\nu,y)-C(x_\nu+z_\nu,x_\nu+z_\nu+r_\nu,y)], \tag{2.35}$$

with $r_\nu=\rho(1+|\nu|+\rho)d/4b$ and

$$C(x,z,y)=\frac14\sum_{n=1}^{\infty}n(2n+x+z+y)\left\{\frac{1}{w_n^-(z)w_n^+(x)[w_n^-(z)+w_n^+(x)]}-\frac{1}{w_n^-(x)w_n^+(z)[w_n^-(x)+w_n^+(z)]}\right\}. \tag{2.36}$$

The symbols x_ν, z_ν, y and $w_n^*(x)$ have the same meaning as below Eqs. (2.32) and (2.33). Equations (2.32) and (2.35) represent our final analytical result for the enhancement of the magnetization due to fluctuations of the order parameter:

$$\delta M = \delta M^{1\infty} + \delta M^{n1} . \tag{2.37}$$

We remark that, at $T = T_c$ and for $Q = 2$, the approximations which led to this result are completely equivalent to the approximations made by KAE in their treatment of isotropic 3D superconductors with finite impurity concentration.

For dirty superconductors, the question of how to evaluate the contributions to the magnetization arising from finite frequency fluctuations has been a matter of controversy. Whereas LP and KAE evaluated the frequency sum in a straightforward manner, MT used the transformation

$$\sum_{\nu=-\infty}^{\infty} g(|\omega_\nu|) = -\frac{2\beta}{\pi}\int_0^\infty d\omega \left(\frac{1}{2} + \frac{1}{e^{\beta\omega}-1}\right) \mathrm{Im}\, g(i\omega) , \tag{2.38}$$

neglected zero-point fluctuations, and evaluated only the term containing the Bose distribution factor. In a recent paper, Maki[16] has investigated the zero-point term (i.e., the term with $\frac{1}{2}$), and he found that it leads to a contribution to the susceptibility which is only weakly dependent on both magnetic field and temperature. He interpreted this contribution as a correction to the Landau diamagnetism of the normal metal due to the electron-phonon interaction. Since in obtaining the experimental results[6] for the fluctuation-enhanced magnetization a weakly temperature-dependent background was subtracted, Maki argues that one has to omit the contribution of the zero-point fluctuations in order to describe the experiments adequately. In fact, Gollub *et al.*[6] reported that the theory of Maki and Takayama nicely explains their experimental results on dirty superconductors, whereas the theories of LP and KAE fail seriously in this limit.

The fact that in the limit of clean isotropic superconductors the susceptibility shows a weak logarithmic temperature dependence well above T_c has been overlooked by LP and KAE, but was pointed out recently by Aslamazov and Larkin.[26] In Appendix B we show that the contribution of the zero-point term to the susceptibility in the clean limit, too, is a slowly varying function of temperature, being finite at T_c and leading to the logarithmic behavior well above T_c. Thus, according to Maki's argument, this contribution should be subtracted in the clean limit, too. But, on the other hand, the magnitude of the zero-point contribution decreases with decreasing impurity concentration, and the effect of subtracting it is far less dramatic in the clean limit than in the dirty limit.

In the layer-compound case the situation is very similar. Even in the 2D limit ($\eta = 0$), where the zero-point fluctuations lead to a contribution to the magnetization which is logarithmically divergent at T_c, its temperature dependence is very weak compared to that of the leading term, which diverges as $(T - T_c)^{-1}$ (cf. Ref. 13).

We therefore evaluate the frequency sums in Eqs. (2.32) and (2.35) following the procedure proposed by MT. Using the relation

$$-\frac{2\beta}{\pi}\int_0^\infty d\omega\, \tfrac{1}{2}\mathrm{Im}\, g(i\omega) = \frac{\beta}{2\pi}\int_{-\infty\cdot i}^{\infty\cdot i} d\omega\, g(|\omega|) \tag{2.39}$$

and $\omega_\nu = 2\pi i\nu/\beta$, we can formulate this summation procedure as follows: Replace

$$\sum_{\nu=-\infty}^{\infty} f(|\nu|)$$

by

$$\sum_{\nu=-\infty}^{\infty}\left(f(|\nu|) - \int_{-1/2}^{1/2} dx f(|\nu+x|)\right) . \tag{2.40}$$

This improves the convergence of the summation considerably, suppressing the high-frequency contributions which might have been taken into account poorly by our preceding approximations.

D. Critical temperature and critical field

The zero-field critical temperature T_c of the present theory according to Eq. (2.25) is given by the familiar BCS result for weak coupling superconductors,

$$kT_c = \gamma\hbar\omega_D e^{-1/\lambda N(\mu)} ,$$

and is independent of the interlayer coupling parameter for $2\eta < \mu$, as is seen from Eqs. (2.19) and (2.20). The present theory, which near the phase transition is equivalent to a linearized Ginzburg-Landau (GL) fluctuation theory, predicts the same type of phase transition for both the 2D and the 3D limit. Recently, Doniach and Penrose[17] studied the influence of nonlinear fluctuations of the GL order parameter on the transition temperature. They found that the temperature T_0 at which the free energy is nonanalytical depends logarithmically on η and is always lower than T_c. In the 3D limit this lowering is extremely small and even for $\tilde{\eta}/\mu \sim 10^{-4}$, it is only of the order of a few percent of T_c. But in the 2D limit, $\eta \to 0$, T_0 approaches zero. Since this nonlinear effect becomes important only for extremely small values of η, the present theory is expected to give a reasonable description of real layer-compound superconductors.

If we assume that the effective electron-electron coupling constant $\bar{\lambda}$ (the 3D form) is independent of the layer spacing s, we have to expect from Eq.

(2.20) that the transition temperature T_c increases with decreasing layer spacing. Measurements[18] of the pressure dependence of T_c indeed show this type of behavior for the nonintercalated compounds TaS_2, $TaS_{1.6}Se_{.4}$, and $NbSe_2$. But intercalated layer compounds show no simple connection between transition temperature and spacing of the metallic layers.

The intercalating organics seem to influence strongly the effective electron-electron interaction, and the 2D form of the coupling constant, $\lambda = \bar{\lambda}/s$, which does not lead to an explicit dependence of T_c on layer spacing, seems to be more appropriate to describe these materials.

The upper critical field $H_{c2}(T)$ in the present theory is given by the divergence of the magnetization in the Prange approximation, which according to Eq. (2.33) occurs for

$$x_0 + \tfrac{1}{2} = 0 \ .$$

This defines the function

$$H_{c2}(T) = -\frac{\hbar c}{|e|}\frac{\epsilon(T)}{4\pi kT}\frac{d(1+\rho)}{\xi_0^2}\ , \tag{2.41}$$

which yields a reasonable description of the transition curve for not too low temperatures, say, for $T/T_c \gtrsim 0.7/(1+\rho_c)$ with $\rho_c = \rho(T_c)$. From Eq. (2.41) it follows that

$$T_c \left.\frac{dH_{c2}}{dT}\right|_{T_c} = -\frac{\hbar c}{|e|}\frac{2d}{\pi^2}\frac{1+\rho_c}{\xi_{0c}^2}\ . \tag{2.42}$$

An exact evaluation of formula (2.24) would lead to Eq. (2.42) with $\pi^2(1+\rho_c)^{-1}$ replaced by $7\zeta(3)\chi(\rho_c)$, where $\chi(\rho_c)$ is the Gorkov function.[19] Thus, the error in Eq. (2.42), introduced by the approximation which made the l sum in Eq. (2.26) tractable, vanishes in the dirty limit and is less than 20% in the clean limit.

In terms of the zero-temperature Ginzburg-Landau coherence length $\xi_{GL}(0)$, defined by

$$\frac{2|e|}{\hbar c}T_c\left|\frac{dH_{c2}}{dT}\right|_{T_c} = \xi_{GL}(0)^{-2}\ , \tag{2.43}$$

Eq. (2.42) reads

$$\xi_{GL}(0)^2 = \frac{\pi^2}{4d}\frac{\xi_{0c}^2}{1+\rho_c}\ . \tag{2.44}$$

III. NUMERICAL RESULTS AND DISCUSSION

The final result for the scaled magnetization, given by Eqs. (2.32) and 2.35), depends in two different ways on the special features of the Hamiltonian, Eq. (2.1). First, there is an over-all anisotropy factor $(\tilde{M}_\perp/m)^{1/2}$, and second, there is the parameter $(m/\tilde{M}_\perp)(\xi_0/s)^2 \equiv b_0$, which determines the shape of the resulting curves. It is this parameter, b_0, which distinguishes the present model from a simple anisotropic effective-mass approximation.

In the layer-compound case, b_0 is expected to be small and to vanish in the 2D limit of decoupled layers ($\eta \to 0$), whereas the 3D effective-mass approximation can be obtained from the present model in the opposite limit, $b_0 \to \infty$ (i.e., $s \to 0$). In the effective-mass approximation, the result for the magnetization differs from the corresponding result for isotropic 3D superconductors only through the anisotropy factor $(\tilde{M}_\perp/m)^{1/2}$.

Thus, it is the dependence on b_0 which contains the effect of lowering the dimensionality from three to two which is the interesting one to investigate.

A nice feature of our result for the precursor diamagnetism is that it provides a uniform framework for the discussion of a number of special cases, which correspond to different approximations investigated earlier in the literature.

First, there are the static approximations, which consider only the zero-frequency ($\nu = 0$) contributions and neglect time-dependent fluctuations of the order parameter. Among these the simplest is the Prange approximation, which is obtained from Eq. (2.32) by omitting the second term in the square brackets or, formally, by setting $Q = 0$. The Prange approximation treats only the long-wavelength fluctuations properly and is expected to be applicable only immediately above the transition.

The "local static" approximation, to be mentioned next, takes into account the momentum dependence of the pair propagator more carefully than the Prange approximation, and, therefore, gives a more realistic description of short-wavelength fluctuations. Equation (2.32) with $\nu = 0$ and finite Q provides an approximation of this type, which, in fact, is very similar to the PAW theory[8] with (at $T = T_c$) $E = (\pi^2/2Q)\hbar^2/(4m\xi_{GL}(0)^2)$ playing the role of their cut-off energy (for a discussion of this cutoff, see Ref. 6).

As discussed by LP and by KAE, the local approximation does not describe the action of a magnetic field correctly. At least for clean superconductors, it is important to include nonlocal effects caused by the latter. The "nonlocal static" approximation, defined by Eqs. (2.32) and (2.35) with $\nu = 0$, takes care of this.

A second class of approximations takes dynamical fluctuations of the order parameter into account. The different approaches used by LP and KAE and by MT, have been discussed at the end of Sec. II D. The MT approximation is obtained from Eq. (2.32) for $Q = 0$ together with the rule (2.40) for the evaluation of the frequency sum. Finally, the "nonlocal dynamic" approximation is defined by Eqs. (2.32), (2.35), and (2.40).

A. Field dependence of the magnetization at T_c

The theoretical results are dicussed most easily at $T = T_c$, where the scaled magnetization defined

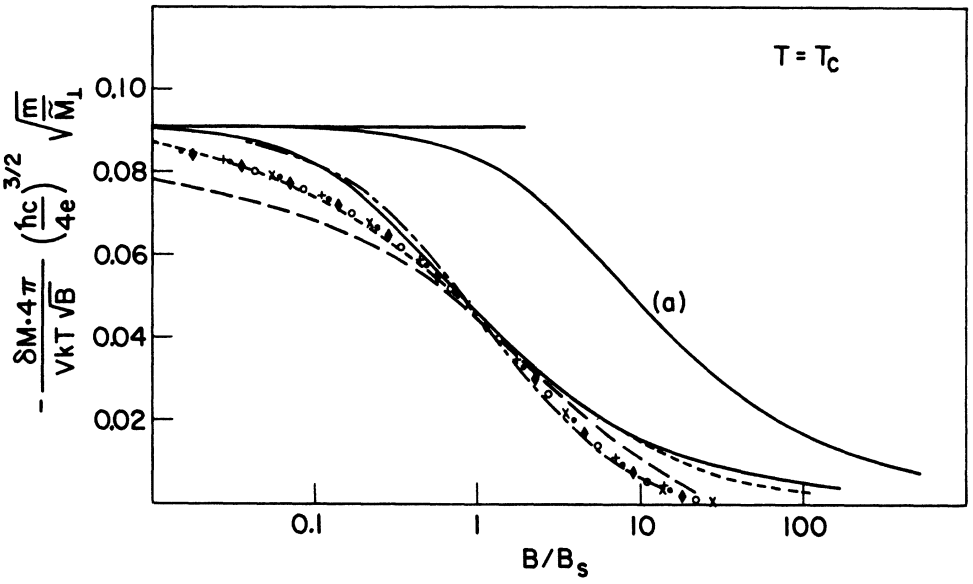

FIG. 2. Curve (a) shows the scaled magnetization in the Prange approximation plotted vs $\pi(\tilde{M}_\perp/m)Bs^2/\phi_0$. The other curves show the scaled magnetization as function of the scaled field B/B_s. In the 3D limit, the numerical results for different impurity concentrations $\rho=0$: (○); $\rho=1$: (×); $\rho=4$: (◆); $\rho=8$: (●); $\rho=16$: (+) follow very closely the same universal curve. For comparison, the clean-limit results of KAE (dotted line) and the experimental results of GBT (dashed line) are also indicated. The solid line refers to nearly 2D layer compounds, and the dash-dot line to a layer-compound intermediate between 2D and 3D behavior.

by Eqs. (2.32) and (2.35) depends only on the scaled magnetic field $b=\xi_0^2|e|B/\hbar c=\pi B\xi_0^2/\phi_0$ with $\phi_0=hc/2|e|$ the flux quantum.

In the Prange approximation the scaled magnetization is a function only of the ratio[20] $b/b_0=\pi(\tilde{M}_\perp/m)Bs^2/\phi_0$. Figure 2 displays a semilogarithmical plot of this function, which has the value 0.0913 at $b/b_0=0$ and decreases with increasing field. At $b=b_s\approx 11.7b_0$, it is depressed to half its zero-field limit, which agrees with the constant 3D results.

In the 2D limit ($b_0=0$), the Prange approximation predicts at T_c a magnetization independent of the magnetic field. In this limit a plot like that in Fig. 2 becomes meaningless.

Each of the improvements of the Prange approximation discussed above yields a curve for the scaled magnetization, which is progressively depressed below the Prange curve as the magnetic field increases. On a semilogarithmical plot like that of Fig. 2 these curves all look very similar. With increasing field b, they decrease slowly (with limit zero for $b\to\infty$) in such a manner that the fall from 80 to 20% of the zero-field limit stretches over about two decades in b, and they can be well characterized by the field value b_s at which they assume half the zero-field limit.

Figure 3 shows $b_s/(1+\rho)=\pi B_s\xi_0^2/\phi_0(1+\xi_0/l)$ as a function of the impurity concentration for the different approximations in the 3D limit (actually for $b_0=100$, $d=3$, and $Q=2$). This type of figure has been presented previously by GBT.[6]

The results shown in Fig. 3 were calculated using the formulas derived in Sec. II in order to test the approximations involved. The agreement with the results given by GBT is good even in the

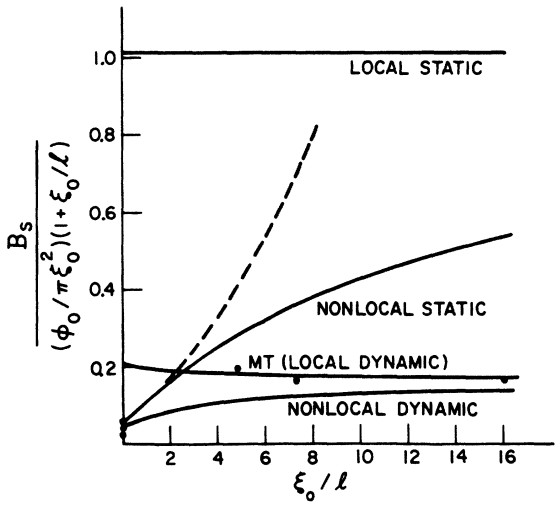

FIG. 3. Impurity dependence of the scaling field B_s in the 3D limit as predicted by the different approximations discussed in the text. The dashed line indicates the result of a straightforward evaluation of the frequency sums (LP-KAE). The points indicate experimental results obtained by GBT.

clean limit ($\rho = 0$), where the approximations of Sec. II are expected to be rather crude.

Comparing their experimental results for the cut-off fields B_s with the predictions of the different approximations, GBT concluded that the most important cut-off mechanism is due to nonlocal effects (LP-KAE theory) for clean superconductors and due to dynamic effects (MT theory) for dirty superconductors.

The present calculations show that the inclusion of both nonlocal and dynamic effects always leads to a smaller cutoff B_s than the inclusion of only one of these effects. In particular, in the clean limit the B_s value predicted by the nonlocal dynamic approximation is smaller than that predicted by the nonlocal static approximation by roughly a factor of $\frac{2}{3}$. This reduced B_s value is in even better agreement with the experimental results for the weak-coupling superconductors In and Nb than the B_s value predicted by the original LP or KAE theory. (The excellent agreement of the LP -KAE cut-off field with the value found experimentally by GBT for the strong-coupling superconductor Pb seems to be accidental.)

Apparently all the B_s values, obtained experimentally by GBT for finite impurity concentrations, are in very good agreement with the local dynamic approximation (MT), whereas the nonlocal dynamic approximation predicts lower values for intermediate impurity concentrations. This discrepancy requires further investigation, and more experimental information about the dependence of B_s on the impurity concentration in the region $1 \lesssim \xi_0/l \lesssim 5$ is desired. But there is no theoretical reason to simply omit the nonlocal effects, and moreover, the nonlocal dynamic approximation is the only one of the approximations discussed, which works reasonably well in both the clean and the dirty limit.

In the layer-compound case the relations between the different approximations discussed above remain qualitatively unchanged. If one defines B_p as the field value at which the magnetization is depressed to half the Prange value,

$$\delta M(B_p) = \tfrac{1}{2}\delta M_{\text{Prange}}(B_p)$$

(note that $B_p = B_s$ in the 3D limit), one obtains, for each value of b_0, qualitatively the same picture as in Fig. 3 with B_s replaced by B_p. Thus, also for layer-compound superconductors the magnetization is depressed below the Prange result, and this depression is mainly due to nonlocal effects in clean materials and due to the dynamics of the fluctuations in dirty ones.

In the following only the results of the nonlocal dynamic approximation will be discussed in more detail.

Since, according to Fig. 3, $b_s/(1+\rho)$ depends only weakly on the impurity concentration, it seems

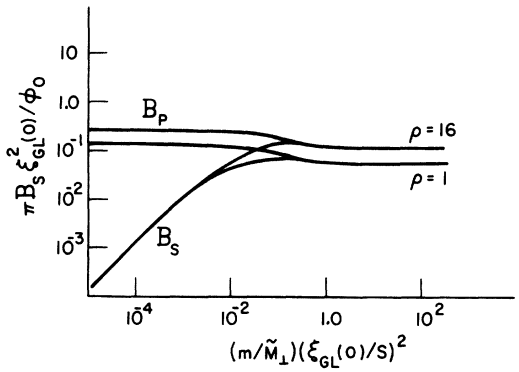

FIG. 4. Dependence of the scaling fields B_s and B_p on the dimensionality parameter $(m/\tilde{M}_\perp)[\xi_{GL}(0)/s]^2$ for two different impurity concentrations.

to be more appropriate to express the magnetic field in terms of

$$b_{GL} \equiv b[\xi_{GL}(0)/\xi_0]^2 = \pi B \xi_{GL}(0)^2/\phi_0$$

than in terms of b itself. Similarly, the dimensionality parameter may be changed to

$$b_0[\xi_{GL}(0)/\xi_0]^2 = (m/\tilde{M}_\perp)[\xi_{GL}(0)/s]^2 = \tfrac{1}{8}\pi^2 r \ ,$$

where r reduces in the dirty limit (and for $T = T_c$) to the dimensionality parameter used by Klemm.[13]

In the nonlocal dynamic approximation the field value B_p, at which the depression of the magnetization below the Prange approximation becomes substantial, depends only weakly on the dimensionality parameter r, being roughly twice as large in the 2D limit as in the 3D limit.

This is shown in Fig. 4 for two values of the impurity concentration, together with the corresponding curves for B_s, the field value at which the scaled magnetization equals one-half of its zero-field limit.[21]

The essential information contained in Fig. 4 is the following. For sufficiently small dimensionality parameter, $r \lesssim 10^{-3}$, the scaled magnetization drops already essentially below its zero-field limit for field values ($B \lesssim 2B_s$), which are so small that the Prange approximation is still valid ($B_s \ll B_p$). This fall is due to dimensionality effects and the scaling field is independent of the impurity concentration ($B_s \approx 3.7(m/\tilde{M}_\perp)\phi_0/s^2$). For increasing r, the fall of the scaled magnetization takes place at higher field values, where nonlocal and dynamic effects become more and more important and limit the scaling field B_s by its 3D value.

Figure 5 shows these results in more detail. The thin solid lines represent the result in the nonlocal dynamic approximation for two values of the impurity concentration and for four different r values. The thick solid lines refer to the 2D limit $r = 0$, and the broken lines indicate the correspond-

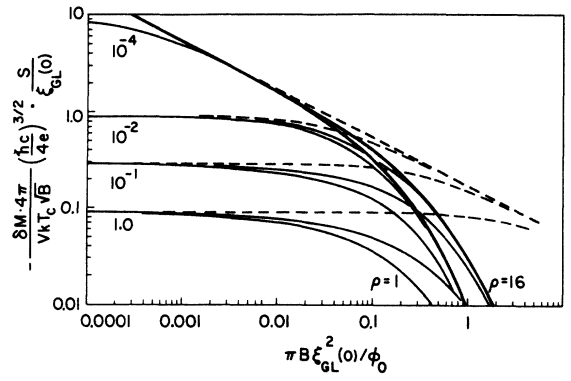

FIG. 5. Field dependence of the scaled magnetization for two different impurity concentrations ($\rho=1$, 16). The thin lines represent the results for four values of the dimensionality parameter, $(m/\tilde{M}_\perp)[\xi_{GL}(0)/s]^2=1$, 0.1, 10^{-2}, and 10^{-4}, and the thick lines represent the corresponding results in the 2D limit. The broken lines refer to the results of the Prange approximation.

ing results in the Prange approximation.

In this double-logarithmic plot the 2D Prange result appears as a straight line with slope $-\frac{1}{2}$. Whereas the curves for $r\sim 1$ look very similar to the corresponding curves in the 3D limit (the main difference being only a scaling factor), the curves for $r\sim 10^{-4}$ show clearly 2D behavior for $\pi B\xi_{GL}^2(0)/\phi_0 \gtrsim 0.002$, and the magnetization itself remains nearly constant while the field increases by one order of magnitude.

Unfortunately, this feature will not show up in the usual semilogarithmical plot of the scaled magnetization as function of B/B_s. This can be seen from Fig. 2, where the solid line represents the scaled magnetization as function of B/B_s in the Prange approximation, which coincides in the field region shown with the result of the full calculation for sufficiently small r ($r\lesssim 10^{-3}$, $B_s \ll B_p$). The shape of this curve is apparently not very different from the results in the 3D limit (actually for $r=100$, $d=3$, $Q=2$), which are shown in Fig. 2 for five different impurity concentrations, and which scale with a remarkable accuracy to a single universal curve. This universal behavior is in agreement with the experimental results of GBT.[6] But the shape of the experimental curve, indicated by the dashed line, does not agree too well with that of the theoretical curve.

For $B<B_s$, the result of the present calculation is in good agreement with the theoretical curve obtained by KAE[10] for clean 3D superconductors (dotted line). But in contrast to the KAE result and in qualitative agreement with the dirty-limit results of MT[11] and Klemm,[13] our 3D curve falls slightly below the experimental curve for $B>B_s$. The value of the scaled magnetic field at which the magnetization practically vanishes is in good agreement with the experimental value.

Considered as a function of the dimensionality parameter r, the shape of the scaled magnetization curve does not change monotonically between the 3D form and the 2D form. The nonlocal and dynamic corrections, which become substantial for $B\sim B_s^{3D}$, always diminish the result of the Prange approximation. For $r\sim 10^{-2}$, the result of the Prange approximation drops to half its zero-field limit in the same field region. In this case, the full calculation leads to a curve which drops more rapidly, exceeding the 2D curve slightly for $B<B_s$ and falling a little below the 3D curve for $B>B_s$. This extreme behavior is indicated in Fig. 2 by the dashed and dotted line.

At the present time, there are no experimental data on the field dependence of the fluctuation-induced magnetization of layer-compound superconductors available, which could be compared with the present results. But we have to expect that such data, if plotted as in Fig. 2, would lead to a curve similar to the experimental curve for isotropic 3D superconductors, and there is little hope that the present theory could be checked unambiguously, or that the dimensionality parameter r could be determined from the *shape* of an experimental curve in the semilogarithmical plot of Fig. 2.

On the other hand, the value of the scaling field B_s itself should provide a much better possibility to measure the dimensionality parameter than the shape of an experimental curve. From Fig. 4 it can be seen that the value of B_s is determined by dimensionality rather than nonlocal or dynamic effects, if $r\lesssim 0.01$, or

$$\tilde{M}_\perp/m \gtrsim 100[\xi_{GL}(0)/s]^2 .$$

Deviations from the 3D behavior should be observable if and only if this condition is fulfilled. On the other hand, if one finds experimentally $B_s \ll 0.1\phi_0/\pi\xi_{GL}(0)^2$, then one has detected dimensionality effects, and one can identify $r\approx 0.2B_s \times\xi_{GL}(0)^2/\phi_0$[or $(\tilde{M}_\perp/m)s^2\approx(11.7/\pi)\phi_0/B_s$].

B. Temperature dependence of the magnetization for finite magnetic field

In the Prange approximation, the scaled magnetization defined by Eq. (2.32) depends on temperature only via $2x_0=-H_{c2}(T)/B$ [cf. Eq. (2.41)]. Near the transition curve, the leading term is given by

$$-\frac{\delta M^{Pr}4\pi}{VkT\sqrt{B}}\left(\frac{\hbar c}{4|e|}\right)^{3/2} = \frac{1}{4}\left(\frac{\tilde{M}_\perp}{m}\right)^{1/2}\left(\frac{y}{(x_0+\frac{1}{2})(x_0+\frac{1}{2}+y)}\right)^{1/2} \qquad (3.1)$$

with $y = b_0/b = (m/\tilde{M}_\perp)\phi_0/\pi B s^2$. Since

$$2x_0 + 1 \approx -\left(\frac{dH_{c2}}{dT}\right)_{T_c(B)} [T - T_c(B)]/B$$

for T near $T_c(B)$, this yields the well-known power laws for the susceptibility, $\chi \sim [T - T_c(B)]^{-1/2}$ and $\chi \sim [T - T_c(B)]^{-1}$ in the 3D limit and in the 2D limit, respectively. But, as seen from Eq. (2.33), the limiting form, Eq. (3.1) is the dominant contribution only if $x_0 + \frac{1}{2} \ll 1$. In the opposite limit, $x_0 + \frac{1}{2} \gg 1$, Eq. (2.33) can be evaluated by replacing the sum by an integral. The result can be written in the form of Eq. (3.1) but with $\frac{1}{4}$ replaced by $\frac{1}{24}$.

The zero-field critical temperature T_c corresponds to $x_0 = 0$. Thus, near T_c even the Prange approximation does not predict a simple power law behavior of the susceptibility, in either the 3D limit or the layer compound case.

For finite r, the scaled magnetization approaches the 3D form near the transition curve, i.e., for $x_0 + \frac{1}{2} \ll y$, but with increasing temperature it is progressively depressed below the 3D curve and approaches the 2D form for $x_0 + \frac{1}{2} \gg y$. The condition $x_0 + \frac{1}{2} = fy$ defines a curve[22]

$$H_D(T) = H_{c2}(T) + 2f(m/\tilde{M}_\perp)(\phi_0/\pi s^2) , \qquad (3.2)$$

in the B-T plane, which separates the region of 2D behavior from that of 3D behavior. In the zero-field limit, the condition $H_D(T) = 0$ defines a characteristic temperature

$$\frac{T_D - T_c}{T_c} = 4f \frac{m}{\tilde{M}_\perp} \frac{\xi_{GL}(0)^2}{s^2} , \qquad (3.3)$$

marking the transition from 2D to 3D behavior. Equation (3.3) agrees with a formula given previously by Lawrence and Doniach[3] ($f = 1$).

The effect of nonlocal and dynamic corrections is to depress the scaled magnetization progressively below the Prange value as the temperature increases. Figure 6 demonstrates that for all values of the dimensionality parameter r this effect is important in the temperature region $T \gtrsim T_c$.

The curves shown are for the fixed value $\pi B \xi_{GL}(0)^2/\phi_0 = 0.0173$, which corresponds to $B \approx 0.3 B_s$ for $\rho_c = 1$ and $r \sim 100$ (3D limit). In this plot the curves for $\rho_c = 16$ lie a little above those for $\rho_c = 1$ at high temperatures. For finite r, the curves approach the 2D form ($r = 0$) at high temperatures and the 3D form as T approaches the transition temperature $T_c(B)$. The power-law predictions of the Ginzburg-Landau theory are found to hold only in the small temperature regime $0 < |dH_{c2}/dT|_{T_c(B)}[T - T_c(B)]/B \lesssim 0.01$.

Figure 7 shows numerical results for several values of r, ρ_c, and B with B/B_s fixed, where B_s is the impurity-dependent scaling field defined in Sec. III A. The temperature is measured in units

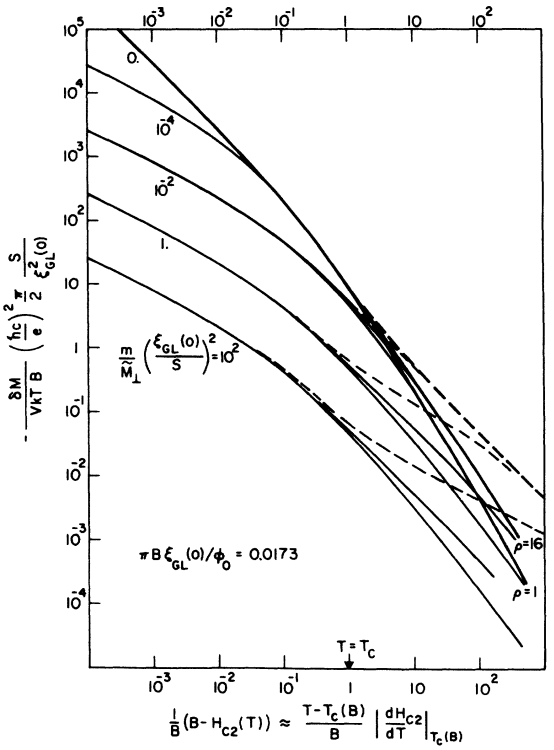

FIG. 6. Temperature dependence of the susceptibility for constant magnetic field. The thin lines show the results for four values of the dimensionality parameter $(m/\tilde{M}_\perp)[\xi_{GL}(0)/s]^2$ (10^2, 1, 10^{-2}, and 10^{-4}), and for two values of the impurity concentration ($\rho = 1$, 16). The thick lines refer to the 2D limit, and the broken lines to the results of the Prange approximation.

of $(T - T_c)|dH_{c2}/dT|_{T_c}/B$, which is the linear approximation of $2x_0$ near T_c.[23] In Fig. 7(a) the results of the present calculation for the 3D limit are compared with the experimental data on In obtained by GBT, and with the results of the MT theory, i.e., the local dynamic approximation defined previously, with x_0 replaced by its linear approximation near T_c. Without this linearization, the result of the local dynamic approximation falls somewhat below the MT curves, but remains significantly above the result of the full calculation for $\rho = 16$. (This indicates that the suppression of high momentum fluctuations is of some importance even in dirty superconductors.)

Whereas the present results in the clean limit are in rather good agreement with the experimental data on In, both for low and high fields, the dirty limit ($\rho = 16$) results lie, in agreement with Klemm's result, noticeably above the In curves, more for $B \approx 5 B_s$ and less for $B \approx 0.3 B_s$. Whether this apparent breakdown of universality is a shortcoming of the theories based on Maki's procedure for the evaluation of frequency sums, or indicates

a measurable effect, is hard to decide at the moment, because data on dirty materials in high fields are not available.

Figure 7(b) shows the calculated results for $\rho = 1$ and several values of the dimensionality parameter. Apparently, the curves depend only weakly on r. Only the high-field curve for $r \lesssim 10^{-4}$ is shifted upwards, because here B_s is so small that the falloff is determined only by dimensionality effects (Prange approximation) and not by the nonlocal and dynamic corrections, which cause the other curves to decrease more rapidly.

As was the case for the field dependence, the temperature dependence of the magnetization is thus expected to show roughly the same universal behavior for layer-compound superconductors as for 3D isotropic superconductors. Therefore, the shape of the curves in the usual plots of the scaled magnetization versus reduced field or temperature seems to be not appropriate to discover dimensionality effects. Moreover, only low-field measurements are available for layer compounds at present,[24] and B_s is not known experimentally.

C. Zero-field susceptibility

In the limit of vanishing magnetic field, Eq. (2.32) yields

$$\lim_{B\to 0}\left[-\frac{\delta M^{\mathrm{loc}}}{VBkT}\frac{\pi}{2}\left(\frac{\hbar c}{e}\right)^2\left(\frac{m}{\tilde{M}_\perp}\right)^{1/2}\frac{1}{\xi_0}\right]=\sum_{\nu=-\infty}^{\infty}\sqrt{b_0}\left[\tilde{F}(\tilde{x}_\nu, b_0)-\tilde{F}(\tilde{x}_\nu+\tilde{z}_\nu, b_0)\right], \tag{3.4}$$

with $\tilde{x}_\nu = x_\nu b$, $\tilde{z}_\nu = z_\nu b$, [x_ν and z_ν are defined below Eq. (2.32)] and

$$\tilde{F}(x, y) = \tfrac{1}{24}[x(x+y)]^{-1/2}. \tag{3.5}$$

Equation (2.35) changes in the same way, with

$$\tilde{C}(x, z, y) = \frac{1}{4}\frac{z+x+y}{z-x}\left(\frac{1}{z-x}\ln\frac{z+\frac{1}{2}y+[z(z+y)]^{1/2}}{x+\frac{1}{2}y+[x(x+y)]^{1/2}}-\frac{2}{[z(z+y)]^{1/2}+[x(x+y)]^{1/2}}\right). \tag{3.6}$$

From Eq. (2.41) it follows that $\tilde{x}_0 = -(|e|/2\hbar c)\xi_0^2 H_{c2}(T)$. Near T_c this may be expressed in terms of the Ginzburg-Landau coherence length:

$$\tilde{x}_0 \approx \frac{1}{4}\left(\frac{\xi_{0c}}{\xi_{\mathrm{GL}}(0)}\right)^2\frac{T-T_c}{T_c} \equiv \frac{1}{4}\left(\frac{\xi_{0c}}{\xi_{\mathrm{GL}}(T)}\right)^2.$$

Thus, the Prange approximation for the zero-field susceptibility near T_c leads to

$$\chi_0^{(\mathrm{Pr})} \equiv \lim_{B\to 0}\frac{\delta M^{(\mathrm{Pr})}}{VB} = -\frac{kT_c}{6\pi}\left(\frac{e}{\hbar c}\right)^2\left(\frac{\tilde{M}_\perp}{m}\right)^{1/2}\left\{\xi_{\mathrm{GL}}(T)\Big/\left[1+\frac{1}{4}\frac{\tilde{M}_\perp}{m}\left(\frac{s}{\xi_{\mathrm{GL}}(T)}\right)^2\right]^{1/2}\right\}. \tag{3.7}$$

This formula has been obtained previously by Lawrence and Doniach,[3] and it reduces to Schmid's[4] results for three and for two dimensions in the limit $s \to 0$ and in the limit $\tilde{M}_\perp/m \to \infty$, respectively.

In Fig. 8(a) numerical results for the susceptibility based on the present theory are compared with the corresponding data given by Klemm.[13] The dirty-limit curve ($\rho = 16$) decreases more slowly with increasing temperature than the curve for $\rho = 1$. Thus, as for finite magnetic field, the present theory predicts no strictly universal behavior of the temperature dependence of the zero-field susceptibility in the 3D limit.

Figure 8(b) shows the results for $\rho = 1$, and several values of the dimensionality parameter r. For $r \geq 1$, the curves coincide with that of the 3D limit, and also the curves for $r = 0.1$ and $r = 0.01$ differ only slightly from this limiting form. Experimental results by PBS[2] on TaS_2 (pyridine)$_{1/2}$ single-phase crystals are also indicated in Fig. 8(b). The material parameters[25] yield $r \lesssim 0.15$, so that nearly 3D behavior must be expected for this material.

Figure 9 shows the numerical results for χ_0 (for $\rho = 1$ and $\rho = 16$) together with the predictions of the Lawrence-Doniach formula, Eq. (3.7), for several values of the dimensionality parameter r in the temperature region $1.002 < T/T_c < 2$. Nonlocal and dynamic effects depress the curves with increasing temperature progressively below the curves given by Eq. (3.7).

This depression sets in at lower temperatures for small impurity concentration ρ_c, and at higher temperatures for larger ρ_c, and it is more effective in the 3D limit than in the nearly 2D case. For $r > 0.1$ the full calculation yields only a very weak dependence of the curves on r, although for $r = 0.1$ the result of the formula (3.7) falls already remarkably below its 3D limit for $T \geq 1.2T_c$. (For $r = 0.01$, the "full" curves start falling essentially below their 3D limit at $T \approx 1.05T_c$.)

For $r \leq 0.001$ the curves show 2D behavior in the region $T > 1.01T_c$, i.e., curves with different r but

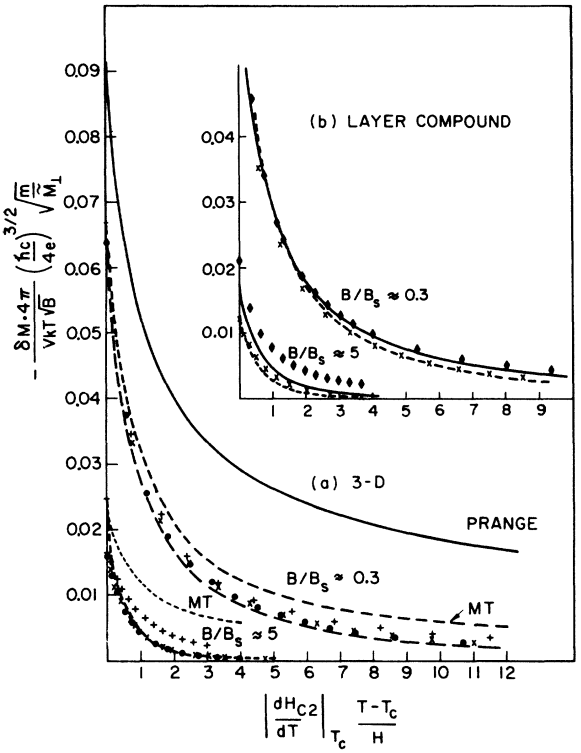

FIG. 7. Temperature dependence of the scaled magnetization for constant magnetic field. (a) Three-dimensional limit: The numerical results for three values of the impurity concentration [$\rho = 0$ (●), $\rho = 1$ (×), and $\rho = 16$ (+)] are shown together with experimental results of GBT (thick broken line) and the predictions of the MT theory (thin broken line) and of the Prange approximation (solid line). (b) Layer compounds: Results are shown for $\rho = 1$ and for four values of the dimensionality parameter $(m/\tilde{M}_\perp)[\xi_{GL}(0)/s]^2$ [10^2, i.e., 3D limit: solid line; 1 : (✕); 10^{-2} : broken line; 10^{-4} : (◆)].

the same ρ_c value coincide if they are multiplied with $r^{-1/2}$. Furthermore, below $T = 1.1T_c$ there is a remarkably large region, where the susceptibility varies essentially as $(T - T_c)^{-1}$.

Such a Curie-Weiss–type behavior of the susceptibility is predicted by the Lawrence-Doniach formula for $(T - T_c)/T_c \gtrsim 50r$. But the theory shows that the inverse susceptibility, varying like $(T - T_c)^{1/2}$ near T_c, increases much faster with increasing temperature for T well above T_c. Thus, even in the 3D limit, there may occur a temperature region below $2T_c$, where the inverse susceptibility varies nearly linear with $T - T_c$.

Figure 9 shows that the extent and the position of this Curie-Weiss–like region depend on the dimensionality parameter r and the impurity concentration ρ_c as well. For $\rho_c = 1$, it is located roughly about $0.1 < (T - T_c)/T_c \leq 0.3$ for $r \geq 0.1$, and it moves to lower temperatures with decreasing r. Since for larger ρ_c the result of the full calculation comes closer to that of the Lawrence-Doniach approximation, the extent of the Curie-Weiss range increases with increasing impurity concentration, and for larger ρ_c its position is shifted towards higher temperatures.

For $r \lesssim 0.01$, the present theory indicates that the temperature dependence of the zero-field susceptibility should differ from the 3D form, and that the value of r can be estimated from the temperature T_D, at which $\chi_0(T - T_c)^{1/2}$ is depressed to one-half of its limit at T_c.

The qualitative predictions of the present theory seem to be in agreement with the experimental results. The apparent similarity of the data on the 3D superconductor Pb-5% Tl with those on the layer compound $TaS_2(\text{pyridine})_{1/2}$ for temperatures with $(T - T_c)/T_c \lesssim 0.2$, which has been observed by Beasley and reported in Klemm's paper, can be understood if $r \gtrsim 0.1$. Reasonable values for the material parameters[25] yield indeed $r = 0.15$. Moreover, if one evaluates the incorrect 2D form of Eq. (3.7) for $r = 0.15$ and for $(T - T_c)/T_c = 0.05$ (which is well within the Curie-Weiss–like regime of the PBS results), the result for the susceptibility appears to be larger than the result of the full calculation by a factor 6.4. This resolves the discrepancy mentioned in Ref. 2. Furthermore, PBS found that mixed-phase samples showed a Curie-Weiss–like behavior over a larger temperature interval than single-phase samples. This would be consistent if mixed-phase samples are dirtier than single-phase samples.

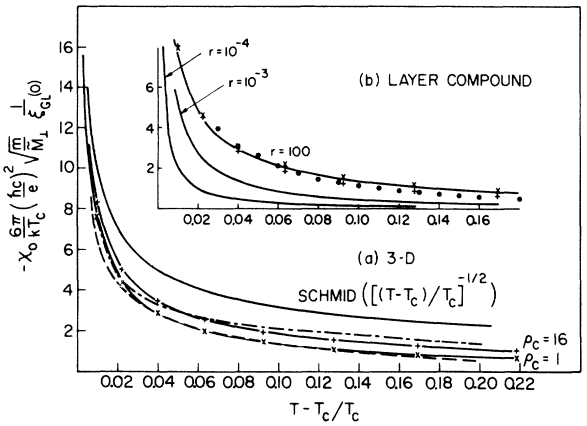

FIG. 8. Zero-field susceptibility. (a) Three-dimensional limit: The results for two values of the impurity concentration [$\rho = 1$: (✕); $\rho = 16$: (+)] are shown together with the experimental curve (dashed) and the theoretical curve (dash-dot) of Klemm's paper (Ref. 13). The result of the Schmid theory is also indicated. (b) Layer compounds: The curves shown refer to three values of the dimensionality parameter ($r = 100$, $r = 10^{-3}$, and $r = 10^{-4}$). Also indicated are the results for $r = 0.1$(×) and $r = 10^{-2}$ (+). The circles represent experimental results of PBS (Ref. 2) on TaS_2 (pyridine)$_{1/2}$ (Ref. 25).

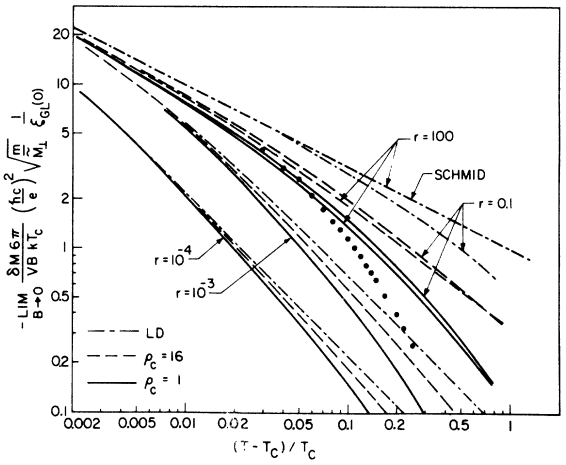

FIG. 9. Zero-field susceptibility for two values of the impurity concentration ($\rho=1$: solid lines, $\rho=16$: dashed lines) and several values of the dimensionality parameter r. Also shown is the prediction of the Lawrence-Doniach formula (dash-dot lines), which for $r=100$ coincides with the 3D Schmid result. The circles indicate experimental results of PBS. (Ref. 2).

Apart from the fact that the present theory in the 3D limit yields values for the scaling fields B_s, which are only in mediocre agreement with experimental values for intermediate impurity concentrations, the main difference between theoretical and experimental results occurs in the temperature dependence of the susceptibility. Whereas the calculated susceptibility, especially in the 3D dirty limit decreases relatively slowly with increasing temperature even after Maki's[16] "zero-point term" has been subtracted, the measured susceptibility is forced to vanish at a temperature slightly above $2T_c$ by the subtraction procedure used by the experimentalists.[6]

ACKNOWLEDGMENTS

It is a pleasure to thank Professor S. Doniach for suggesting the subject of this work and for many stimulating and helpful discussions during its progress. I also wish to thank him and Professor W. Harrison for their obliging and generous hospitality. Furthermore, I appreciate gratefully a scholarship granted by the Deutsche Forschungsgemeinschaft and the hospitality extended to me by the Department of Applied Physics, Stanford University, Stanford, California.

APPENDIX A

It is well known[15] that the one-particle Green's function

$$G_\sigma(\vec{r}, t; \vec{r}', t') = -iT\langle\psi_\sigma(\vec{r}, t)\psi_\sigma^\dagger(\vec{r}', t')\rangle , \quad \text{(A1)}$$

corresponding to the 3D limit of the Hamiltonian equation (2.4), is diagonal in the Landau representation,

$$G_\sigma(\vec{r}, t; \vec{r}', t) = \sum_\alpha \phi_\alpha(\vec{r}) G_\sigma(\alpha; t-t')\phi_\alpha^*(\vec{r}') , \quad \text{(A2)}$$

where

$$\phi_\alpha(\vec{r}) = (\text{const.})e^{i(yk_y+zk_z)}\varphi_n(x-X)$$

are the eigenfunctions of a particle with charge $-|e|$ in the vector potential $\vec{A}(\vec{r}) = (0, Bx, 0)$. The quantum numbers are $\alpha = (n, k_y = -X/R^2, k_z)$ with $R = (|e|B/\hbar c)^{-1/2}$ the magnetic length. Furthermore, $G_\sigma(\alpha) = G_\sigma(n, k_z)$ is known to be independent of k_y.

To prove Eq. (A2), one uses the symmetry properties of the Hamiltonian: rotations around the B axis and arbitrary translations change the Hamiltonian in the same way as certain gauge transformations of the vector potential do.

Thus, the Hamiltonian is invariant under such a symmetry transformation and a suitable subsequent gauge transformation. From this it is easily seen that the Green's function has the symmetry property

$$G(\vec{r}, t; \vec{r}', t') = \exp[-i(|e|/2c\hbar)(\vec{r}-\vec{r}')\cdot\vec{A}(\vec{r}+\vec{r}')] \times \tilde{G}((x-x')^2+(y-y')^2, |z-z'|; t-t') , \quad \text{(A3)}$$

which is sufficient[15] to prove the diagonality stated in Eq. (A2). [$\vec{A}(\vec{r})$ is a linear function of its argument $\vec{r}$.]

Similarly, the pair propagator, Eq. (2.6), satisfies

$$L(\vec{r}, t; \vec{r}', t') = \exp[-i(|e|/c\hbar)(\vec{r}-\vec{r}')\cdot\vec{A}(\vec{r}+\vec{r}')] \times \tilde{L}((x-x')^2+(y-y')^2, |z-z'|; t-t') , \quad \text{(A4)}$$

with

$$\tilde{L}((x-x')^2+(y-y')^2, |z-z'|; t-t') = L[\tfrac{1}{2}(\vec{r}-\vec{r}'), t; -\tfrac{1}{2}(\vec{r}-\vec{r}'), t'] . \quad \text{(A5)}$$

Therefore, the pair propagator is diagonal in the Landau representation for a doubly charged particle:

$$L(\vec{r}, t; \vec{r}', t') = \sum_\alpha \Psi_\alpha(\vec{r}) L_\alpha(t-t')\Psi_\alpha^*(\vec{r}') , \quad \text{(A6)}$$

where $\Psi_\alpha(\vec{r})$ is obtained from $\phi_\alpha(\vec{r})$ by replacing e by $2e$, and where $L_\alpha = L_{n,k_z}$ is independent of k_y.

In the presence of randomly located impurities, these arguments remain valid for the impurity average of the propagators, if the impurity potential is cylindrical symmetric about the magnetic field direction.

In the ladder approximation, the pair propagator is determined by the equation[14]

$$L(1, 2) = \Pi(1, 2) - i\lambda\int d3L(1, 3)\Pi(3, 2) , \quad \text{(A7)}$$

where

$$1=(\vec{r}_1, t_1)\,, \quad \int d3=\int_0^{-i\beta} dt_3 \int_{\vec{r}_3}\,,$$

and

$$\Pi(\vec{1}, 2)=G_\sigma^0(\vec{r}_1, t_1; \vec{r}_2, t_2)G_\sigma^0(\vec{r}_1, t_1; \vec{r}_2, t_2) \tag{A8}$$

with G_σ^0 the free single-particle Green's functions ($\bar{\lambda}=0$).

In the Ψ_α representation this simplifies to

$$L_\alpha(l)=\Pi_\alpha(l)-i\bar{\lambda}L_\alpha(l)\Pi_\alpha(l)\,, \tag{A9}$$

with

$$\Pi_\alpha(l)=\int_{\vec{r}}\int_{\vec{r}'}\frac{i}{\beta}\sum_{l'}\Psi_\alpha^*(\vec{r})G_\sigma^0(\vec{r}, \vec{r}'; \zeta_{l'})$$

$$\times G_\sigma^0(\vec{r}, \vec{r}'; \zeta_{l-l'-1})\Psi_\alpha(\vec{r}') \tag{A10}$$

and $\zeta_l=\mu+i(2l+1)\pi/\beta$, where Fourier coefficients with respect to the imaginary time dependence were taken as usual. In the presence of impurities, Eq. (A10) has to be replaced by Eqs. (2.8) and (2.9). This is the result of the usual perturbation theory, taking into account only "s-wave" scattering (lifetime independent of quantum numbers) and neglecting all diagrams which contain any crossing impurity and/or interaction lines.

The contributions of pair fluctuations to the grand canonical potential, Eq. (2.5), are easily expressed in terms of the pair propagator:

$$\delta\Omega=\int_0^\lambda\frac{d\lambda}{\lambda}\langle H_1\rangle=\int_0^{\bar{\lambda}}d\bar{\lambda}\int_{\vec{r}}L(\vec{r}, 0; \vec{r}, 0^+)\,. \tag{A11}$$

This can be written

$$\delta\Omega=\int_0^{\bar{\lambda}}d\bar{\lambda}\,\frac{i}{\beta}\sum_l\sum_\alpha L_\alpha(l)\,, \tag{A12}$$

and leads, with Eq. (A9), immediately to Eq. (2.7). Of course, the considerations of this Appendix apply to the case of a layer compound in a homogeneous magnetic field perpendicular to the layer planes as well as to the three-dimensional limit, since they depend only on the cylindrical symmetry of the problem.

APPENDIX B

To calculate the susceptibility for small magnetic field B in the clean limit, we evaluate the sum over Landau quantum numbers n in the free-energy formula, Eq. (2.7), by means of the Euler-MacLaurin formula and neglect terms of the order $O(B^4)$. Since for small B the main contributions come from large n, we can use the asymptotic formula [see Ref. 10, Eq. (2.34)]

$$\tfrac{1}{2}(-1)^n\int_0^\infty du\,e^{-u/2}L_n(u)g(u)$$

$$=g(\tilde{u})+2\,\frac{\partial^2}{\partial\tilde{u}^2}g(\tilde{u})+\tfrac{4}{3}\tilde{u}\,\frac{\partial^3}{\partial\tilde{u}^3}g(\tilde{u})+\cdots\Big|_{\tilde{u}=4n+2}$$

to obtain, with Eqs. (2.8) and (2.11),

$$\Pi_{nk_z}=\Pi(y, k_z)+\left(\frac{\pi B}{\phi_0}\right)^2\left[2\,\frac{\partial^2}{\partial y^2}+\frac{4}{3}\,y\,\frac{\partial^3}{\partial y^3}\right]$$

$$\times\Pi(y, k_z)+\cdots\Big|_{y=(4n+2)/R^2}\,, \tag{B1}$$

where

$$\Pi(k_x^2+k_y^2, k_z)=kT\sum_l Q(k_x^2+k_y^2, k_z)$$

is the zero-field form [cf. Eqs. (2.8) and (2.12)]. With Eq. (B1) the evaluation of the free energy [neglecting terms $O(B^4)$] is straightforward, although somewhat tedious. The result for the zero-field susceptibility can be written

$$\chi_0=\lim_{B\to0}\left(-\frac{1}{VB}\frac{\partial\Omega}{\partial B}\right)=\frac{1}{3\pi}\frac{kT}{\phi_0^2}\sum_\nu\int d^3k$$

$$\times\frac{y[(\partial/\partial y)\bar{\lambda}\Pi(y, k_z; \nu)]^3}{[1-\bar{\lambda}\Pi(y, k_z; \nu)]^3}\Big|_{y=k_x^2+k_y^2}\,. \tag{B2}$$

This formula can also be obtained from Eq. (2.31), using first Eq. (2.14), then the local approximation Eq. (2.13), and, finally, the Euler-MacLaurin formula to evaluate the n sum.

In the 3D isotropic case $\Pi(k_x^2+k_y^2, k_z)=\Pi(k^2)$, and Eq. (B2) can be simplified:

$$\chi_0=\frac{8kT}{9\phi_0^2}\sum_\nu\int_0^\infty dk\,\frac{k^4[(\partial/\partial k^2)\Pi(k^2; \nu)]^3}{[\bar{\lambda}^{-1}-\Pi(k^2; \nu)]^3}\,. \tag{B3}$$

This formula has been obtained by Aslamazov and Larkin[26] within their diagrammatic approach.[27] To evaluate Eq. (B2), we proceed as in Eqs. (2.23)–(2.26), with Eq. (2.24) replaced by

$$I(k_x^2+k_y^2, k_z; l, \nu)^{-1}=2l+1+|\nu|$$

$$+\frac{1}{d}\,\frac{\tilde{\epsilon}(k)/(\hbar^2/2m\xi_0^2)}{2l+1+|\nu|}\,, \tag{B4}$$

the limit for vanishing magnetic field and vanishing impurity concentration. $\tilde{\epsilon}(\vec{k})$ is given by Eq. (2.18). We obtain

$$1-\bar{\lambda}\Pi(k_x^2+k_y^2, k_z; \nu)=\bar{\lambda}N(\mu)\left\{\ln\frac{T}{T_c}+\mathrm{Re}\psi\left[\frac{1+|\nu|}{2}+\frac{i}{2}\left(\frac{\tilde{\epsilon}(\vec{k})}{d\hbar^2/2m\xi_0^2}\right)^{1/2}\right]-\psi(\tfrac{1}{2})\right\}$$

$$\approx\bar{\lambda}N(\mu)\left[\ln\frac{T}{T_c}+\frac{1}{2}\ln\left((1+|\nu|)^2+\tfrac{7}{2}\zeta(3)\,\frac{\tilde{\epsilon}(\vec{k})}{d\hbar^2/2m\xi_0^2}\right)\right]\,. \tag{B5}$$

With this result, and in the effective-mass approximation ($d=3$), Eq. (B2) can be written in the form of Eq. (B3) and finally simplified to

$$\chi_0^{3D} = -\tfrac{1}{9}[\tfrac{7}{12}\zeta(3)]^{1/2}\frac{kT\xi_0}{\phi_0^2}\left(\frac{\tilde{M}_\perp}{m}\right)^{1/2}\sum_{\nu=-\infty}^{\infty}\int_0^\infty dx\,\frac{x^4}{[(1+|\nu|)^2+x^2]^3\{\ln(T/T_c)+\frac{1}{2}\ln[(1+|\nu|)^2+x^2]\}^3}\,. \tag{B6}$$

Since $kT\xi_0=\hbar v_F/2\pi$, independent of T, the temperature dependence occurs only via $\ln(T/T_c)$. For T close to T_c, Eq. (B6) can be evaluated asymptotically, and the leading term ($\nu=0$) yields just the Schmid result [cf. Eq. (3.7)]. With increasing T, χ_0^{3D} decreases monotonically and approaches for large T the "zero-point" term, which is obtained from Eq. (B6) by replacing $\sum_\nu$ by $2\int_0^\infty d\nu$. Since the main contributions to the x integral come from the region $1+|\nu|\lesssim x\lesssim 3(1+|\nu|)$, the x integral can be done for large $\ln(T/T_c)$, leaving

$$2\int_0^\infty d\nu\,\frac{3\pi}{16}\frac{1}{1+\nu}\left[\ln\frac{T}{T_c}+\ln(1+\nu)+\tfrac{1}{2}\ln C\right]^{-3} = \frac{3\pi}{16}\left[\ln\frac{T}{T_c}+\tfrac{1}{2}\ln C\right]^{-2}, \tag{B7}$$

where $C\approx 5$. This is essentially the high-temperature behavior of the 3D zero-field susceptibility obtained by Aslamazov and Larkin. The $\ln^{-2}(T/T_c)$ behavior should, however, not be taken too seriously. It was obtained for $\ln T/T_c \gg 1$, and is due to high-frequency contributions [the integral in Eq. (B7) converges poorly]. At these high temperatures neither the neglect of the frequency cutoff nor the Gorkov theory itself are justified. Nevertheless, Eq. (B6) clearly shows the weak logarithmic temperature dependence of the susceptibility well above T_c.

To estimate the magnitude of the zero-point term for T close to T_c, we may approximate the integral over ν and x roughly by

$$2\int_0^{\nu_0} d\nu\int_0^\infty dx\,\frac{x^4}{(1/T_c-1+\nu+\frac{1}{2}x^2)^3} = 3\pi\sqrt{2}\left[\left(\frac{T-T_c}{T_c}+\nu_0\right)^{1/2}-\left(\frac{T-T_c}{T_c}\right)^{1/2}\right], \tag{B8}$$

where ν_0 is of the order of unity. We see that the zero-point contribution is finite at T_c and that its temperature dependence is much weaker than that of the dominant ($\nu=0$) term, which diverges like $(T-T_c)^{-1/2}$ at T_c.

To include the effect of finite magnetic field, we may replace $\tilde{\epsilon}(\vec{k})$ in Eq. (B5) by $\tilde{\epsilon}(\vec{k})+b\hbar^2/(m\xi_0^2)$ [cf. Eq. (2.24)], which yields $H_{c2}(T)+H_{c2}(0)[1-(T/T_c)^2]$ with $H_{c2}(0)=d\phi_0/[7\pi\zeta(3)\xi_{0c}^2]$ [cf. remarks below Eq. (2.24)]. Inserting this in the Euler-MacLaurin expansion of the susceptibility, we find that the correction terms are of order $(B/H_{c2}(0))(T_c/T)^2$. Thus, for $B\ll H_{c2}(0)$ the susceptibility is given by Eq. (B6) with T_c replaced by $T_c(B)$. We can use this result to estimate the effect of the "zero-point" term on the scaling field B_s. KAE obtain $b_s=3B_s/7\zeta(3)H_{c2}(0)\approx 0.05$ or $B_s\approx 0.14H_{c2}(0)$. Then, with $(T_c(B_s)-T_c)/T_c\approx 0.1$ the contribution of the zero-point term to $\delta M(T_c,B)/\sqrt{B}$ for $B=B_s$ is of the order of 10% to 20% of the KAE result. Subtraction of the zero-point term will thus reduce the scaling field noticeably, in agreement with our numerical result.

For finite impurity concentration, Eqs. (B2) and (B5) must be modified and the temperature dependence of the susceptibility becomes less obvious. It can be shown, however, that for finite impurity concentration the temperature dependence of the zero-point term is weaker than in the clean limit. Thus, the MT-subtraction procedure is well justified for isotropic 3D superconductors with arbitrary impurity concentration.

In the 2D limit, the zero-point contribution to the susceptibility calculated from Eqs. (B2) and (B5) diverges like $\ln[T_c/(T-T_c)]$. This variation with temperature is still weak as compared with the $(T-T_c)^{-1}$ divergence of the leading Schmid term. The high temperature variation of susceptibility and zero point term is obtained as $\sim(T_c/T)\ln^{-3}(T/T_c)$ for $\ln T/T_c\gg 1$, in agreement with Ref. 26. Thus, in the 2D limit it depends on the experimental situation whether the subtraction of the zero point term is feasible. If a temperature dependent fluctuation susceptibility can be resolved experimentally only for temperatures close to T_c, as, e.g., in the layer compound measurements of Ref. 2, the subtraction is justified. But if the fluctuation susceptibility could be measured accurately up to temperatures well above T_c, say, $T>2T_c$, care must be taken.

Our model for layered compounds shows an intermediate behavior, being 3D near T_c and changing over to a 2D behavior at sufficiently high temperatures. The temperature dependence of the zero-point term is weaker for finite impurity concentration than in the clean limit.

Thus the MT-subtraction procedure apparently is a useful hypothesis in order to compare theory and experimental results on both layered and isotropic superconductors with arbitrary concentration of impurities.

*Supported by the Deutsche Forschungsgemeinschaft.
†Some aspects of this work have been supported by U. S. Army Research Office, Durham, N. C.
‡On leave of absence from Institut für Theoretische Physik der Universität zu Köln, 5 Köln, Germany.

[1]T. H. Geballe, A. Menth, F. J. Di Salvo, and F. R. Gamble, Phys. Rev. Lett. 27, 314 (1971).
[2]D. E. Prober, M. R. Beasley, and R. E. Schwall, *Proceedings of the Thirteenth International Conference on Low Temperature Physics, Boulder, Colorado*, 1972, edited by R. H. Kropschot and K. D. Timmerhaus (University of Colorado Press, Boulder, Colo., 1973).
[3]W. E. Lawrence and S. Doniach (unpublished).
[4]A. Schmid, Phys. Rev. 180, 527 (1969).
[5]H. Schmidt, Z. Phys. 216, 336 (1968).
[6]J. P. Gollub, M. R. Beasley, and M. Tinkham, Phys. Rev. Lett. 25, 1646 (1970); J. P. Gollub, M. R. Beasley, R. Callarotti, and M. Tinkham, Phys. Rev. B 7, 3039 (1973).
[7]R. E. Prange, Phys. Rev. B 1, 2349 (1970).
[8]B. P. Patton, V. Ambegaokar, and J. W. Wilkins, Solid State Commun. 7, 1287 (1969).
[9]P. A. Lee and M. G. Payne, Phys. Rev. Lett. 26, 1537 (1971); Phys. Rev. B 5, 923 (1972).
[10]J. Kurkijärvi, V. Ambegaokar, and G. Eilenberger, Phys. Rev. B 5, 868 (1972).
[11]K. Maki and H. Takayama, J. Low Temp. Phys. 5, 313 (1971).
[12]W. E. Lawrence and S. Doniach, *Proceedings of the Twelfth International Conference on Low Temperature Physics, Kyoto, Japan*, 1970 (Academic Press of Japan, Kyoto, 1971), p. 361.
[13]R. A. Klemm, M. R. Beasley, and A. L. Luther, Phys. Rev. B 8, 5072 (1973).
[14]See V. Ambegaokar, in *Superconductivity*, edited by R. D. Parks (Marcel Dekker, New York, 1969), p. 259.
[15]J. Sher and T. Holstein, Phys. Rev. 148, 598 (1966); H. Keiter, Z. Phys. 198, 215 (1967).
[16]K. Maki, Phys. Rev. Lett. 30, 648 (1973).
[17]S. Doniach and O. Penrose, Bull. Am. Phys. Soc. 18, 385 (1973).
[18]T. F. Smith, R. N. Shelton, and R. E. Schwall, Bull. Am. Phys. Soc. 18, 385 (1973); T. H. Geballe (private communication).
[19]See N. R. Werthamer, in Ref. 14.
[20]Klemm uses the notation $2b/b_0 = 1/\sigma$.
[21]The B_s curves show a maximum near $r = 0.1$, where the crossover from 2D to 3D behavior occurs. Such a slight enhancement above the 3D value was also obtained in the local dynamic approximation and is, therefore, not a typical effect of nonlocal electrodynamics. Klemm's results apparently do not show this behavior.
[22]The numerical factor f is of the order of unity. For $f \approx 6$, $H_D(T_c)$ is the field value, at which the scaled magnetization in Prange approximation is depressed due to dimensionality effects to half its 3D value.
[23]In the numerical calculations the temperature dependence of the cut-off parameter Q, defined in Eq. (2.29), was approximated by $Q(T) = Q(T_c)\psi'(\frac{1}{2} - \epsilon(T)/4\pi kT)/\psi'(\frac{1}{2})$. In the temperature range shown in Fig. 7 the effect of this temperature dependence was practically of no importance.
[24]Recently, the reliability of the measurement by Geballe *et al.* (Ref. 1) has been questioned. [T. H. Geballe (private communication); cf. also Ref. 2].
[25]The data are taken from the χ' vs T curve for single-phase samples at $H_\perp = 3$ Oe (cf. Ref. 2). The material parameters are assumed to be $T_c = 3.43$ °K, $s = 12$ Å, $\xi_{GL}(0) = 190$ Å, and $(m/\tilde{M}_\perp)^{1/2} = 0.023$. The latter value is chosen in agreement with recent experiment [R. E. Schwall (private communication)], but it may be only an upper limit because of a remaining uncertainty in the value of $dH_{c2_\parallel}/dT$. Then, the resulting dimensionality parameter is $r \lesssim 0.15$.
[26]L. G. Aslamazov and A. I. Larkin, in Proceedings of the U. S.-U. S. S. R. Symposium on Current Topics in the Theory of Condensed Matter, University of California, Berkeley, California, 1973, (unpublished).
[27]L. G. Aslamazov and A. I. Larkin, Fiz. Tverd. Tela 10, 1104 (1968) [Soviet Phys.-Solid State 10, 875 (1968)].